Journal of proteome research

Article

pubs.acs.org/jpr

Cytotoxic and Proinflammatory Effects of Metal-Based Nanoparticles on THP-1 Monocytes Characterized by Combined Proteomics Approaches

Nataliya K. Tarasova,[†] Audrey Gallud,[‡] A. Jimmy Ytterberg,[†,§] Alexey Chernobrovkin,[†] Jaime Ruiz Aranzaes,[⊥] Didier Astruc,[⊥] Alexei Antipov,[¶] Yuri Fedutik,[¶] Bengt Fadeel,[‡] and Roman A. Zubarev*[,†]

[†]Division of Physiological Chemistry I, Department of Medical Biochemistry and Biophysics, [‡]Nanosafety & Nanomedicine Laboratory, Division of Molecular Toxicology, Institute of Environmental Medicine, and [§]Rheumatology Unit, Department of Medicine, Karolinska Institutet, Solna, 17177 Stockholm, Sweden

[⊥]Université de Bordeaux 1, CNRS UMR, 5255 Talence, France

[¶]PlasmaChem GmbH, Rudower Chaussee 29, D-12489 Berlin, Germany

Supporting Information

ABSTRACT: Thorough characterization of toxic effects of nanoparticles (NP) is desirable due to the increasing risk of potential environmental contamination by NP. In the current study, we combined three recently developed proteomics approaches to assess the effects of Au, CuO, and CdTe NP on the innate immune system. The human monocyte cell line THP-1 was employed as a model. The anticancer drugs camptothecin and doxorubicin were used as positive controls for cell death, and lipopolysaccharide was chosen as a positive control for proinflammatory activation. Despite equivalent overall toxicity effect (50 ± 10% dead cells), the three NP induced distinctly different proteomics signatures, with the strongest effect being induced by CdTe NP, followed by CuO and gold NP. The CdTe toxicity mechanism involves down-regulation of topoisomerases. The effect of CuO NP is most reminiscent of oxidative stress and involves up-regulation of proteins involved in heat response. The gold NP induced up-regulation of the inflammatory mediator, NF-κB, and its inhibitor TIPE2 was identified as a direct target of gold NP. Furthermore, gold NP triggered activation of NF-κB as evidenced by phosphorylation of the p65 subunit. Overall, the combined proteomics approach described here can be used to characterize the effects of NP on immune cells.

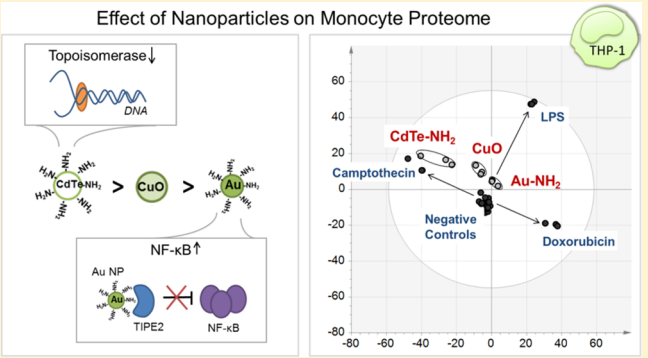

KEYWORDS: *Nanomaterials, anticancer drugs, monocyte assay, inflammation, gold nanoparticles, quantum dots, copper oxide, thermal proteome profiling*

INTRODUCTION

Nanomaterials are being rapidly developed, and the areas of their applications are constantly increasing. In particular, metal and metal oxide nanoparticles (NP) are being produced in increasing amounts for a variety of applications. For instance, copper oxide (CuO) NP have already been successfully applied in gas sensors, batteries, catalysis, high temperature superconductors, field emission emitters, and solar energy conversion.[1] Moreover, these NP were demonstrated to have antimicrobial properties.[2] Biomedical applications of NP are also emerging, the currently most promising areas being drug delivery and medical imaging. Gold (Au) NP are an example of potential drug delivery agents,[3] while cadmium telluride (CdTe) NP and other quantum dots (QD) are widely used fluorescent probes for biomolecular and cellular imaging.[4]

The use of new substances in industry and especially in medicine requires understanding the biological impact of these materials and careful estimation of possible toxicity effects.[5] Different methods can be applied to assess and understand the influence of various compounds, including NP, from morphological and functional characterization to investigation of the genes and protein pathways involved in the response. In the current study, we applied a proteomics approach that combines three recently developed methods. The first approach, which we have designated as functional identification of protein target by expression proteomics (FITExP),[6] is based on the "central dogma of proteomics" and postulates that the proteins (or their post-translational modifications) most intimately involved in a

Received: August 16, 2016
Published: December 15, 2016

DOI: 10.1021/acs.jproteome.6b00747
J. Proteome Res. 2017, 16, 689−697

biological mechanism will be most up-or down-regulated when this mechanism sets on. In FITExP, cancer cells are treated by a panel of drugs, and the protein expression changes are analyzed in terms of regulation, specificity, and exclusivity to identify the most likely drug target. The second approach is the proteomics-based monocyte assay for prediction of the innate immune system response to a novel stimulus.[7] The assay employs THP-1 monocytic cell line and requires positive controls (treatment by activating or differentiating stimuli), while treatment with a buffer is used as a negative control. The positive controls for this study were lipopolysaccharide (LPS) and two anticancer drugs with known mechanisms of action. LPS was selected to account for the possible proinflammatory component of the cell response to NP, while anticancer drugs were employed as controls for cell death. The THP-1 cell line originated from monocytic leukemia cells,[8] which make anticancer drugs appropriate as controls for cell death. Finally, we applied another recently developed proteomics technique called thermal proteome profiling (TPP) to identify potential drug targets. In this approach, which relies on ligand-induced thermal stabilization of target proteins, cells are cultured with or without drugs (here: with or without NP) of interest and heated to different temperatures to induce protein denaturation, and the remaining soluble proteins are then quantified by mass spectrometry.[9]

There are relatively few examples in the literature of the application of proteomics method to study the cytotoxicity of nanoparticles on cells.[10] Studies using monoblastic leukemia cells (U937) revealed that the multiwalled carbon nanotubes (MWCNT) induce biological responses in these cells, in part due to impurities, such as iron.[11] The response was characterized by alteration in abundances of proteins involved in metabolism, biosynthesis, response to stress, and cell differentiation. In another study, mass spectrometry was applied to assess the proteome changes in human hepatocellular carcinoma cells (HepG2) confronted with singe-walled CNTs or graphene oxide.[12] The study showed that SWCNT induced oxidative stress and interfered with several cellular processes including metabolic pathways, while GO was less cytotoxic with only moderate changes in protein expression. Furthermore, the analysis of the secretome of MWCNT-exposed human monocyte-derived macrophages showed release of inflammation-related and lysosomal proteins, with induction of apoptosis in the case of long, rigid MWCNT.[13]

For the present study, we selected three metal-based NP with different toxicity potency estimated by half maximal effective concentration, that is, EC_{50} values using THP-1 cells (Gallud et al., manuscript in preparation). Thus, all three NP induced cell death in THP-1 cells, but the same effect was achieved at different concentrations. The selected NP are cadmium telluride NP functionalized with amine groups (CdTe-NH_2), gold NP, also with amine groups attached (Au-NH_2), and copper oxide NP without surface coating (CuO-core). CdTe NP, used in the core of highly luminescent quantum dots (QDs), are known to have toxic effects in biological systems.[14] QDs are especially toxic to cultured cells under UV illumination for prolonged time due to photolysis induced by released Cd^{2+} ions.[15] It has been demonstrated that QDs can enter the cells through endocytosis. Surface coating was shown to affect the uptake of the particles thus influencing their cytotoxicity. QDs can transfer absorbed optical energy to nearby oxygen molecules to generate reactive oxygen species (ROS) such as free radicals and superoxide and singlet oxygen, which results in cell damage and death.[16] Oxidative stress was also found to be a primary toxic effect of CuO NP.[17] These NP can enter the cytoplasm through diffusion across the membrane or endocytosis.[1] Inside the cells, Cu^{2+} ions can be released, which would induce ROS production or chelate formation with biomolecules resulting in inactivation of the latter. Besides the core component, the toxic effects of NP can also depend on their size and surface charge. For instance, 1.4 nm gold nanospheres triggered necrosis, mitochondrial damage, and induced oxidative stress in several cell lines, possibly due to the intercalation with DNA in the cell nucleus. However, no evidence was found for cellular damage in case of 15 nm gold nanospheres.[18] In another study, cationic gold NP were found to be toxic while anionic were not.[19]

The aim of the current study was to investigate the toxicity of the selected nanomaterials by contrasting them with known toxicity mechanisms of anticancer drugs. To enable a side-by-side comparison of the proteomes of NP- and drug-treated cells, THP-1 monocytes were treated with both types of agents at the concentrations inducing death in half of the cell population (EC_{50}).

MATERIALS AND METHODS

Nanoparticles

The CuO and CdTe-NH_2 NP were dispersed in sterile phosphate buffer saline (PBS), and the Au-NH_2 NP were dispersed in 1.5 mM KCl solution at concentration of 5 mg/mL with sonication (5 min, 40 kHz, ice-cold water bath). The physicochemical characteristics of CuO-core, CdTe-NH2, and Au-NH_2 are summarized in Table 1. The primary particle size of the NP was measured by transmission electron microscopy (TEM). The hydrodynamic size was estimated by dynamic light scattering (DLS) or differential centrifugal sedimentation (DCS). The CdTe-NH_2 had the emission wavelength of about 590 nm. NP were characterized in dH_2O.

Table 1. Physicochemical Characterisation of NP

#	nanoparticle	primary particle size, nm (TEM[a])	hydrodynamic size ± SD, nm
1	CdTe−NH_2	<4	55.6 nm (DCS[b])
2	Au−NH_2	10−20 and 32−54 (bimodal)	
3	CuO-core	10−20	1408.3 ± 101.5 (DLS[c])
			152.7 ± 3.8 (DCS)

[a]TEM, transmission electron microscopy. [b]DLS, dynamic light scattering. [c]DSC, differential centrifugal sedimentation.

Limulus Amebocyte Lysate (LAL) Assay

NP were assessed for potential endotoxin contamination following the QCL-1000 End point Chromogenic LAL Assay (Lonza) protocol. The enzymatic reaction was performed on NP alone, NP in the presence of LPS or NP in the presence of LPS, and polymyxin B (PolyB), an LPS inhibitor. Briefly, the stock suspensions of NP were diluted at 100 μg/mL in endotoxin-free culture medium and 50 μL of each suspension were dispensed into a 96-well plate. LPS and PolyB were added at 1 EU/mL or 5 μM, respectively, followed by 1 h incubation at RT. The reaction was initiated by first adding the proenzyme and then the substrate. After 16 min, a stop solution of acetic acid 25% v/v in distillated water was added, and the absorbance

DOI: 10.1021/acs.jproteome.6b00747
J. Proteome Res. 2017, 16, 689−697

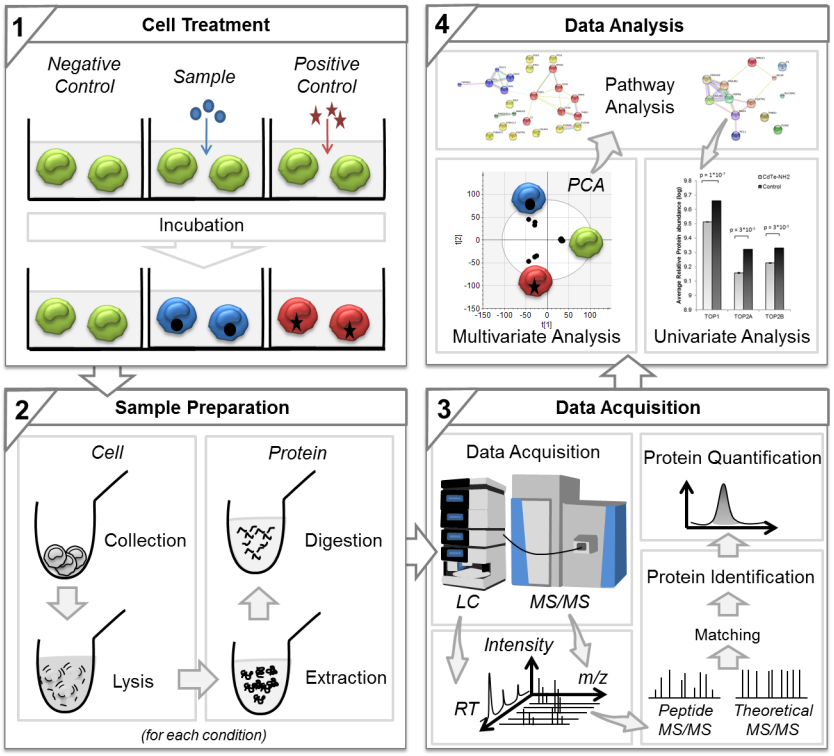

Figure 1. Workflow for characterization of the responses of THP-1 cells. Proteomics-based monocyte assay.

was read at 405 nm using an Infinite 200 Tecan microplate reader operating with the Magellan v7.2 software.

Proteomics-Based Monocyte Assay

The workflow of the proteomics-based monocyte assay, presented in Figure 1, consists of four main steps: (1) cell treatment with compounds of interest (in the current study: CuO-core, CdTe-NH_2, and Au-NH_2 NP) as well as reference treatments (in the current study: LPS, doxorubicin, and camptothecin), (2) sample preparation for label-free proteomics, (3) data acquisition with LC−MS/MS, and (4) bioinformatics analysis of the data with multivariate, univariate, and pathway analyses.[7] The details of these steps are described further.

Cell Culture, Treatment, and Counting

The human monocytic cell line THP-1 was cultured in RPMI-1640 medium supplemented with 10% heat-inactivated fetal bovine serum (Biochrome, Merck Millipore), 0.05 mM mercaptoethanol, 2 mM L-glutamine, and 100 U/mL penicillin−streptomycin mixture. Treatments and their concentrations are given in Table 2. The experiment was performed in a 24-well plate (Sarstedt) in three replicates.

Table 2. Treatments and Their EC_{50} Concentrations for THP-1 Cells

#	nanoparticle/anticancer drug	EC_{50}[a]	solvent (conc. in well)
1	CdTe−NH_2	5 μg/mL	PBS
2	Au−NH_2	15 μg/mL	KCl (1.5 mM)
3	CuO-core	22 μg/mL	PBS
4	camptothecin	50 μM	DMSO (0.5%)
5	doxorubicin	30 μM	DMSO (0.3%)

[a]EC_{50}, half maximal effective concentration (conc. of the treatment inducing 50% dead cells).

Nonadherent THP-1 cells (10^6 cells/mL) were used in the beginning of the experiment. Lipopolysaccharide (LPS; Sigma) was diluted with PBS. Phorbol 12-myristate 13-acetate (PMA; Sigma) was diluted with dimethyl sulfoxide (DMSO); the final concentration of DMSO in culture was 0.005%. Upon treatment and incubation, the fraction of dead cells was estimated using the cell count with trypan blue, as a marker for cells with damaged membrane; the desired effect of the compound was death in 50 ± 10% cells. The cells in suspension were collected first, while the cells remaining adherent were incubated for 5 min with 0.05% trypsin mixed with EDTA and phenol red (Gibco) before collection. Collected cells were counted using a TC10 cell counter (BioRad) with trypan blue staining. After centrifugation (7 min; 1000*g*), the cell pellets were washed with PBS and lysed in a lysis buffer (8 M urea and 50 mM NaCl in 100 mM ammonium bicarbonate) by sonication on ice (40 s; with pulses; in two repeats with a break in between).

Protein Isolation and Digestion

Cell lysates were centrifuged (20 min; 20 800*g*; 8 °C), and supernatants were collected. The protein concentration in the supernatants was determined using the BCA kit (Pierce). Following reduction (5 mM dithiothreitol, 37 °C, 30 min) and alkylation (14 mM iodoacetamide, RT, 30 min), 10 μg of proteins was digested by trypsin (Promega) at a 1:30 trypsin/protein concentration ratio (37 °C, overnight). Digestion was stopped with formic acid (FA; final concentration 5%). Digests were desalted with Stage Tips (Thermo Scientific), dried, and resuspended in 0.1% FA prior to analysis. In the last experiment, where only adherent cells were analyzed, acetone precipitation of proteins was performed prior to digestion.

DOI: 10.1021/acs.jproteome.6b00747
J. Proteome Res. 2017, 16, 689−697

Mass Spectrometry

LC−MS/MS analyses were performed using a nanoflow HPLC combined with a Q Exactive mass spectrometer (both, Thermo Scientific, Germany). For each sample, 1 μg was injected from a cooled autosampler onto an 25 cm long fused silica tip column (SilicaTips, New Objective Inc., USA) packed in-house with 1.9 μm C18-AQ ReproSil-Pur (Dr. Maisch GmbH, Germany). The chromatographic separation was achieved using an acetonitrile (ACN)/water solvent system containing 0.1% FA with 2% ACN and a gradient of 120 min from 6% to 31% of ACN. Mass spectra were acquired with a resolution of R = 70 000, followed by up to 10 consecutive data-dependent MS/MS spectra taken using higher-energy dissociation (HCD) with the normalized collisional energy (NCE) set at 25 units. Samples were analyzed in a randomized order.

Protein Identification and Quantification

MS/MS data were extracted and processed according to a previously described protocol[7,20,21] and searched against the concatenated version of the UniProt complete proteome database (release 2013_04, 71 434 human protein sequences) using the Mascot search engine v. 2.4 (Matrix Science, UK). The following parameters were used: trypsin digestion with a maximum of two missed cleavages; carbamidomethylation (C) as a fixed modification; pyroglutamate (Q), oxidation (M), and deamidation (N) as variable modifications; a precursor mass tolerance of 10 ppm and a fragment mass tolerance of 0.02 Da. The list of identified proteins was filtered using 1% false discovery rate (FDR) and at least two peptides per protein as limiting parameters. Label-free quantification was performed using the in-house written, open-source program Quanti that compensates in silico for electrospray current fluctuations.[20] In total, 3289 protein groups were quantified in the experiment with at least two unique peptides per protein. Further details and results of the analyses are provided in Supporting Information (Table S-1).

Experimental Design and Statistical Rationale

The label-free proteomics experiment has been performed in three biological replicates for each condition. Protein abundances were normalized to sum of intensities with the assumption that equal amounts of protein digests were injected for each sample. Proteins that likely originated from the media (serum albumin and hemoglobin) or sample handling (keratins) were excluded from the results. Log transformed abundance values were used for further analysis. Principal component analysis (PCA) and orthogonal projections to latent structures (OPLS) were performed using Simca software version 14.0 (Umetrics). Unpaired Student's t test with equal or unequal variance (depending on the result of Excel F-test) was applied to calculate the p-values. FDR (Benjamini−Hochberg)[22] adjusted (q-values) or Bonferroni adjusted p-values (E-values) with a threshold of 5% were used to identify significantly up/down-regulated proteins. Pathway analysis was conducted using String version 10 (http://string-db.org/). The q-values for Gene Ontology (GO) terms enrichment were calculated against the data set with all identified proteins. All the error bars in the figures represent sample standard errors of the mean. Fold change was calculated as a ratio of the average values of biological replicates' results.

Quality control of proteomics data was performed in several ways. (1) The retention times of peptides were compared for consistency among different samples within the same experiment. None of the samples was excluded from the data set. (2) It was checked that the protein abundances correlated with the order of injection. No protein with a correlation better than R^2 > 0.80 was identified. (3) PCA plots were analyzed for the presence of outliers. No outliers were identified. (4) Proteins quantified in less than 80% of all experiments were excluded from the analysis. One protein fulfilling the criterion was removed. (5) To ensure that the drug treatment was performed in a consistent way, FITExP analysis was performed, as described previously.[6] In short, for every quantified protein, its regulation, specificity, and exceptionality were calculated, and the proteins were ranked according to these parameters. The proteins with the lowest sum of the three ranks were considered drug target candidates. The ranks of the known targets (e.g., topoisomerase TOP1 for camptothecin and TOP2 for doxorubicin) were then inspected. With low ranks of the targets, the analysis is deemed successful.

Thermal Proteome Profiling (TPP)

To study proteins potentially interacting with the Au-NH_2 NP, we adopted a recently developed approach termed thermal proteome profiling (TPP).[9] This approach allows identification of changes in protein thermal stability across the proteome with the aid of isobaric tandem mass tag 10-plex (TMT10) reagents and mass spectrometry. THP-1 cells (2×10^6 cells/mL) were incubated with 15 μg/mL Au-NH_2 or 1.5 mM KCl in two replicates for 3 h at 37 °C, collected (2×10^6 cell/tube) and processed according to the TPP protocol.[9] The LC−MS/MS data acquisition and search were performed as described earlier with following modifications: (1) 50 cm long EASY-spray column (Thermo Scientific); (2) gradient of 90 min from 2% to 30% of ACN in two steps; (3) 35 NCE; (4) 35 000 MS/MS resolution; (5) search using MaxQuant.[23] The subsequent bioinformatic analysis, including data normalization, melting curve fitting, and determination of statistical significance of compound−protein interactions, was performed in R (analyzeTPPTR).

NF-κB Activation

NF-κB activity was determined by the NF-κB p65 (pS536) SimpleStep ELISA assayTM (Abcam, Cambridge, MA) according to the manufacturer's instruction. Briefly, THP-1 cells were seeded in 12-well plates at a density of 10^6 cells/mL and exposed for 24 h to Au-NH_2 (15 μg/mL) or LPS (100 ng/mL) or medium alone, in presence or absence of the inhibitor of NF-κB, BAY 11−7082 (5 μM) (Abcam, Cambridge, MA). At the end of the incubation, cells were harvested and washed with PBS. The phosphorylated NF-κB p65 (pS536) protein was quantified based on a horseradish peroxidase-TMB substrate reaction. The absorbance was read at 450 nm using a Tecan Infinite F200 plate reader. Experiments were performed twice in duplicates. One-way analysis of variance (ANOVA) was used for statistical analysis, assuming equal variances at $p < 0.05$.

RESULTS

THP-1 Cell Treatments

Prior to the study, the NP were all confirmed to be endotoxin-free (data not shown), a prerequisite when assessing NP effects on immune-competent cells such as the THP-1 cell line.[24] As a first step, we determined the cytotoxicity of the different NP (CuO-core, CdTe-NH_2, and Au-NH_2) using the vital dye exclusion assay. The concentrations applied were selected to induce approximately 50% cell death (Table 2). The fraction of live cells following treatment is shown in Figure 2.

DOI: 10.1021/acs.jproteome.6b00747
J. Proteome Res. 2017, 16, 689−697

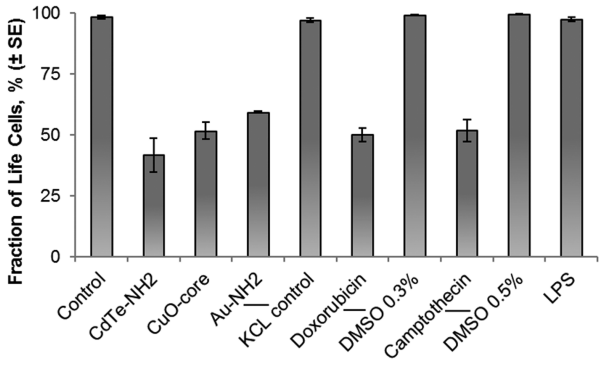

Figure 2. Fraction of live cells following the indicated treatments. The cells were incubated with indicated treatments for 24 h. The fraction of live cells was estimated based on aliquot (10 μL) using automated cell counter with trypan blue staining. "Control" corresponds to treatment with a buffer, while controls for specific treatments are connected to these treatments by horizontal lines. The remaining 990 μL of media with cells was centrifuged, the cell pellets were washed with PBS and analyzed with LC−MS/MS.

FITExP Analysis

Next, samples were collected from THP-1 cells exposed according to the previous section, and LC−MS/MS analyses were performed and data analysis conducted as detailed in the Materials and Methods.

The ranks of the known targets topoisomerase TOP1 in camptothecin treatment and TOP2A in doxorubicin treatment were 469 and 172, respectively, out of 3243 quantified proteins. The low ranks of the targets testify to the adequate cell treatment, sample collection, proteomics analysis, and data processing.

Multivariate Analysis

Multivariate analysis of the proteomics results provides the best overview. PCA (R^2 = 0.71; Q^2 = 0.45) produced six independent components, which is in line with seven main groups present: three NP, two drugs, LPS, and controls. In the PCA plots, the triplicates of the samples representing different treatments are well separated from other triplicates, which testify to the high overall quality of the assay including cell treatment, preparation, and proteomics measurements. The most significant (first) component separates drugs as well as QD treatments from LPS and controls (Figure 3A and Table S-2). The second component differentiates doxorubicin treatment on the one hand and from the QD treatment on the other hand, while the third component distinguishes Au- versus CuO-based NP (Figure 3B). The fourth (Figure 3C) and fifth (Figure 4A) components separate LPS and camptothecin. The negative controls, including cells treated with cell culture medium, DMSO, and KCl (see Figure 1 and Table 2), grouped together, suggest that these solvents did not affect the cells.

Overall, it appears that, despite nearly equivalent biological effect (half of the cells were dead), Au- and CuO-based NP did not produce as strong effects on the THP-1 proteome as the anticancer drugs, while CdTe-NH_2 NP affected the proteome to degree comparable to the drugs. To test further this assumption, an OPLS model was created based on four groups (proteomes of LPS-, doxorubicin-, and camptothecin-treated cells as well as controls), and applied to the proteomes of the NP-treated cells to predict their positions on the same plot (Figure 4B). With such a mapping, the CdTe-NH_2 NP effect appears closest to the cell response to camptothecin, the gold particles are inducing responses in line with the response to LPS, and the CuO-treated cells occupy an intermediate position between LPS activation and camptothecin response. The specific proteins most involved in these responses were identified by univariate analysis.

Univariate and Pathway Analyses

The up- and down-regulated proteins in the treated cells compared to the corresponding controls were identified by *t* test analysis with Bonferroni correction for multiple testing. Proteins with *E*-values (*p*-values multiplied by the total number of quantified proteins) below 0.05 (Table S-3) were selected for further pathway analysis by String.

In the LPS-treated cells, the GO processes 'defense response to other organism' and 'response to lipopolysaccharide' (*q*-value (GO:0098542) = 8×10^{-5} and *q*-value (GO:0032496) = 8×10^{-3}, correspondently) were among the top three enriched GO terms for the up-regulated proteins (with fold change greater than two), which is expected for a bacterial component. A number of the proteins known to play important role in energy metabolism (glucose-6-phosphate dehydrogenase, creatine kinase, and long-chain-fatty-acid—CoA ligase 1) were identi-

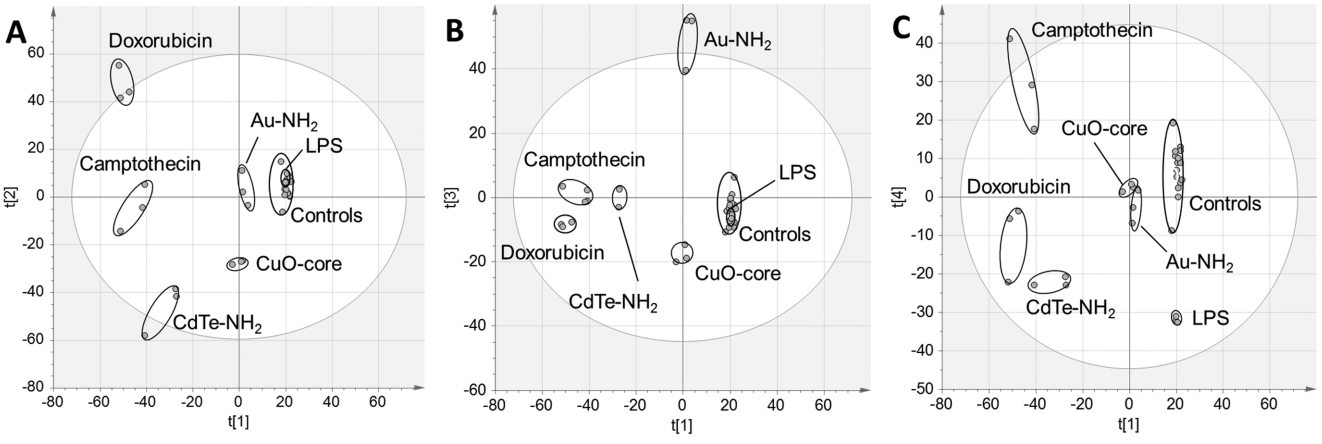

Figure 3. PCA of the proteomes of the treated THP-1 cells and the controls for first four components out of six total. The three biological replicates are encompassed by circles. (A) First component against the second component; (B) first component against the third component; (C) first component against the fouth component.

DOI: 10.1021/acs.jproteome.6b00747
J. Proteome Res. 2017, 16, 689−697

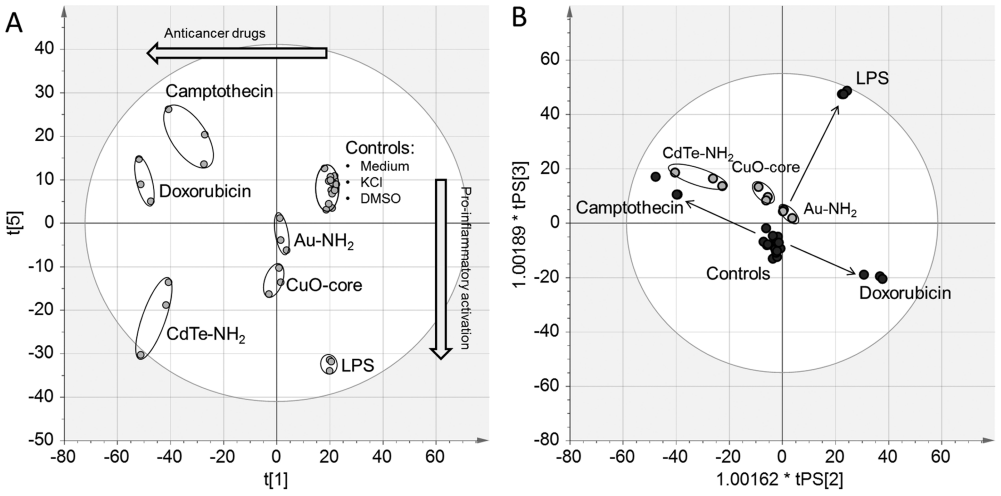

Figure 4. NP characterization and classification based on position on PCA and OPLS plots. (A) PCA of the proteomes of the treated THP-1 cells and controls, first versus fifth components. (B) Prediction of the positions of samples on the score plot based on the OPLS model with four groups (proteomes of LPS-, doxorubicin-, and camptothecin-treated cells as well as controls).

fied to be up-regulated both in LPS-treated cells and cells treated with Au NP. NF-κB (nuclear factor kappa-light-chain-enhancer of activated B cells) were also up-regulated in both these cases, which confirmed proinflammatory response in Au NP-treated cells observed in Figure 4B.

The proteins involved in 'extracellular matrix organization' (GO:0030198) were among the up-regulated proteins in LPS-treated cells as well as in CuO-treated cells (16 and 8 proteins, respectively). This fact correlates with the observation under the microscope that the CuO-core NP treatment induced more adherent cells compared to control, but fewer compared to LPS (data not shown). Moreover, a quarter (26%) of the proteins up-regulated in the CuO-treated cells were associated with immune system processes (GO:0002376). Similar to camptothecin treatment, the proteins involved in the processes 'response to unfolded protein' and 'response to topologically incorrect protein' were up-regulated by CuO-core NP. Unique for this treatment was the up-regulation of a number of proteins involved in 'response to heat' (q(GO:0009408) = 3.4 × 10^{-6}).

The CdTe-NH_2 treatment of THP-1 cells induced more up-regulated proteins in common with camptothecin than with the CuO-core NP treatment (36% vs 20%, respectively). This fact correlates well with the PCA and OPLS data in Figures 3 and 4. Moreover, topoisomerase I, known to the camptothecin target protein, was down-regulated in both camptothecin and CdTe-NH_2 treated cells (Figure 5A). Analysis of different subtypes of topoisomerases revealed that all of them were down-regulated in CdTe-NH_2 treated cells (Figure 5B).

TPP Analysis of Au-NH_2 NP

To further probe the mechanism of NF-κB activation by Au-NH_2 NP, TPP analysis was performed. The TPP approach is almost orthogonal to the expression-proteomics assay described earlier. The only common step in-between the approaches is analysis of peptide mixture with mass spectrometer. The TPP assay is based on the idea that protein binding with its target molecule changes the thermal stability of the protein. This change can be detected as difference in melting curves (fraction of non-denaturated protein versus temperature) of the protein with and without its target. The fraction of non-denaturated protein at each temperature point in the melting curves in the TPP assay is analyzed by multiplexed quantitative mass

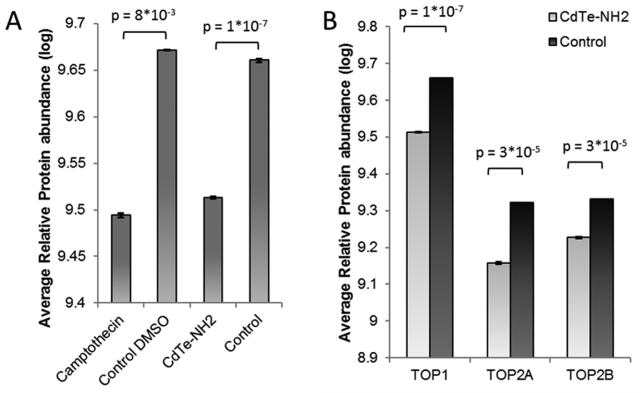

Figure 5. Average relative abundances of topoisomerases. (A) The average relative abundance (log transformed) of topoisomerase 1 (TOP1) in cells treated with camptothecin, control with DMSO, CdTe-NH_2, and control with media. (B) The same for different topoisomerases: 1, 2A (TOP2A) and 2B (TOP2B) in cells treated with CdTe-NH_2 or media ("Control").

spectrometry using isobaric tandem mass tag 10-plex (TMT10) reagents. Further bioinformatics analysis is combined in R package[9] and includes data normalization, melting curve fitting and determination of statistical significance of changes in protein stability.

In total, 4699 protein groups were quantified, for 4673 of which melting curves were generated. Nine protein groups were detected as potential intracellular targets of Au-NH_2 (Table S-4). Tumor necrosis factor (TNF) alpha-induced protein 8-like protein 2 (TP8L2_HUMAN or TIPE2) was identified as a potential target (Figure 6A), and the same protein was also observed to be down-regulated in the assay (Figure 6B; p-value =1 × 10^{-3} or 5 × 10^{-5} if compared to combined control with nine replicates). The melting point of this protein in cells treated with gold NP was on average 2.14 °C higher than in control cells (1.3 standard deviations from median value of melting point differences for all the analyzed proteins). TIPE2 is a negative regulator of NF-kB and is required for maintaining immune homeostasis.[27] This might indicate that the mechanisms triggering NF-κB up-regulation (Figure 6C) in LPS and Au-NH_2 treated cells are different. In case of LPS, innate cells

DOI: 10.1021/acs.jproteome.6b00747
J. Proteome Res. 2017, 16, 689−697

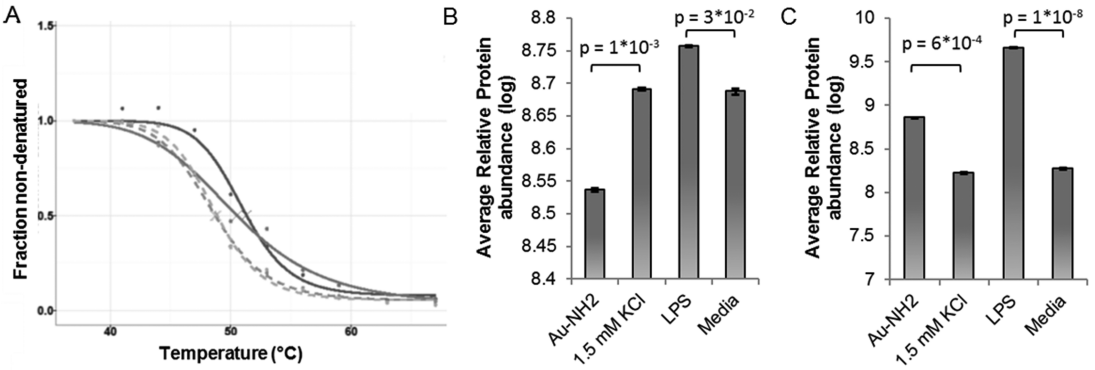

Figure 6. Effect of Au-NH_2 on TIPE2 and NF-κB in THP-1 cells. (A) TPP results, two replicates. Melting curves of the protein TIPE2 in cells treated with Au-NH_2 (solid lines) and with 1.5 KCl as a control (dashed lines). (B) The average relative abundance (log transformed) of TIPE2 (TP8L2_HUMAN) in cells treated with Au-NH_2 and LPS (with corresponding controls: 1.5 mM KCl or media). (C) Same as in panel B, but for NF-κB p100 subunit (NFKB2_HUMAN) protein.

are activated via pattern recognition receptors. In case of Au-NH_2 NP, it is possible that the inactivation of TIPE2 results in NF-κB activation. This suggests a novel mechanism of action of NP.

Gold NP Trigger NF-κB Activation

To provide further evidence for NF-κB activation by Au-NH_2 NP, cells were exposed for 24 h to the particles at the same EC_{50} concentration used for the proteomics studies, and activation of NF-κB was monitored by quantifying the intracellular content of phosphorylated NF-kB p65 protein.[25] LPS and cell culture medium alone were used as positive and negative controls, respectively. Our results showed that LPS triggered significant NF-κB activation, as expected and this was diminished upon preincubation of the cells with the inhibitor BAY-11 7082, which is known to selectively and irreversibly inhibit NF-κB activation by blocking phosphorylation of IκB-α without affecting constitutive IκB-α phosphorylation.[26] Notably, Au-NH_2 also induced significant NF-κB activation, and this was blocked by BAY-11 7082 (Figure 7). A similar effect was observed for smaller (5 nm) Au NP with similar surface functionalization (data not shown).

DISCUSSION

NP are being produced in increasing amounts and represent potential environmental pollutants. The understanding and quantitative assessment of their toxicity are important for protection of human health and the environment, not at least workers who may be at risk of exposure to NP. In the current study, we focused on three metal-based NP using THP-1 monocytes as a model. The CdTe NP as well as their constituent heavy metal ion Cd^{2+} are known to be cytotoxic. In the current study, CdTe-NH_2 NP revealed a proteomics response comparable to that of anticancer drugs, and with a similar effect on topoisomerases, which might indicate that the toxicity mechanism involves alkylation of DNA or effects on chromatin-related proteins. Indeed, previous studies have shown that Cd^{2+} ions, which can be released from NP, can inhibit the DNA repair mechanisms in cells and form charge-mediated interactions with histones in the cell nucleus.[28,29]

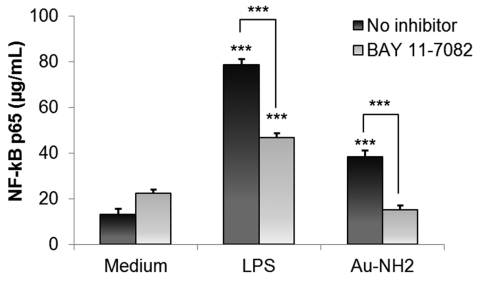

Figure 7. Au-NH_2 NP trigger NF-κB activation in THP-1 cells. THP-1 cells were exposed for 24 h to Au-NH_2 NP (15 μg/mL) in presence or absence of BAY 11−7082 (5 μM), an inhibitor of NF-κB activation. Media alone or LPS (100 ng/mL) were used as negative and positive controls, respectively. The concentration of NF-κB p65 was determined by using a specific ELISA. ***, $p < 0.01$; **, $p < 0.05$, compared to medium alone, or inhibitor.

CuO-core NP are less toxic compared to the CdTe-NH_2 NP and even at a 4.5-times higher dose (that was required to achieve a similar outcome, e.g., 50% death), the effect on the proteome in exposed THP-1 cells was significantly smaller. The proteins up-regulated in CuO-treated cells included four heat shock proteins as well as a number of molecules involved in unfolded protein response. Such effects could potentially be due to Cu^{2+} being able to substitute in proteins other biologically important dications (Fe^{2+}, Mn^{2+}, and Mg^{2+}), causing structural changes in these proteins. Changes induced in extracellular matrix organization, similar to LPS treatment, could be due to monocyte activation as well as to cellular responses to ROS induced by CuO NP.

In contrast to the CuO and CdTe NP, gold NP have been shown to induce cell death only in particular cases, and their cytotoxicity strongly depends on the size and the surface groups and attendant surface charge.[18,19] In general, a positive charge (e.g., an amine group as in the current study) promotes cellular uptake of NP. In our study, the Au-NH_2 NP induced cell death in THP-1 cells (indeed, the study design was such that each NP caused the death of about 50% of the cells), but the proteome response was the weakest among all tested treatments. Thus, it is possible that immune cells can recover more readily after exposure to gold NP[15] than to other NP.

The key inflammatory mediator NF-κB was among the proteins up-regulated in THP-1 cells after exposure to Au-NH_2, and this protein was also up-regulated in LPS-treated cells. Importantly, endotoxin contamination of the NP was excluded in this study. Thus, the monocyte response to gold NP seems proinflammatory, which is consistent with earlier observations

DOI: 10.1021/acs.jproteome.6b00747
J. Proteome Res. 2017, 16, 689−697

that gold NP induce cytokine release by immune cells.[30,31] Moreover, the data obtained with ELISA assay support our findings based on proteomics approaches and verify that the gold NP elicit NF-κB activation. Cell activation is associated with an increased energy use, and gold NP were found to induce up-regulation of the key proteins involved in different energy metabolism pathways, which was also observed in LPS-treated cells. The TPP approach gave an indication that the mechanisms of NF-κB up-regulation in LPS- and gold NP-treated cells might be different. Hence, while LPS triggers Toll-like receptors leading to proinflammatory responses in monocytes, gold NP could act through dysregulation of immune homeostasis. We identified the TIPE2 protein, crucial for intracellular inflammatory homeostasis, and inhibition of NF-κB as targets of gold NP and down-regulated in the treated cells. The changes in abundances of TIPE2 in treated cells compared to untreated were significant on *p*-value level but did not pass the strict Bonferroni correction criteria, and thus this protein was not included in Table S-3. However, even slight externally induced changes in proteins involved in cell homeostasis might lead to significant changes in cells, which is most likely what occurred in gold NP-treated cells. Therefore, potentially, the activation of NF-κB activation in cells treated with gold NP is mediated through weakening the TIPE2 control over this central inflammatory mediator. Previous studies have provided evidence that fullerenes or fullerene derivatives may act as "protein mimics" and interact directly with cellular proteins thereby deregulating their function.[32,33] However, the present study is the first to point toward direct protein binding as a possible mechanism underlying the proinflammatory effects of NP.

Taken together, these studies have implicated specific interactions between nanoparticles and proteins using human immune-competent cells as a model. Identifying such molecular interactions could help to elucidate the biology and toxicology of nanomaterials.[34]

CONCLUSIONS

Even though the overall toxicity effect of the three investigated types of NP was the same (50% cell death), different NP induced distinct and distinguishable proteomics signatures, with the strongest effect being induced by CdTe-NH_2 NP, followed by CuO NP, and with Au-NH_2 showing the weakest effect. The QD toxicity mechanism involves down-regulation of topo-isomerase and is likely due to interference with DNA of chromatin proteins. The effect of CuO-core resembles that of oxidative stress and involves up-regulation of proteins involved in heat response. The gold NP induced up-regulation of the inflammatory mediator NF-κB and a number of proteins related to energy metabolism, consistent with proinflammatory activation. This activation could be induced by immune homeostasis dysregulation mediated by TIPE2. In summary, the combined proteomics approach (proteomics-based monocyte assay, FITExP, and TPP) described here can be used with advantage to characterize and classify the toxic effects of NP on immune cells.

ASSOCIATED CONTENT

Supporting Information

The Supporting Information is available free of charge on the ACS Publications website at DOI: 10.1021/acs.jproteome.6b00747.

Proteomics experiment: data table used for subsequent analysis and parameters of protein sequence search and abundance normalization; parameters of the PCA model in Figure 3A; up- and down-regulated proteins in the treated cells compared to negative control (medium) identified by *t* test with Boenferroni correction; list of potential Au-NH_2 targets according to TPP experiment (XLSX)

AUTHOR INFORMATION

Corresponding Author

*E-mail: Roman.Zubarev@ki.se. Phone: +46 8 524 87594. Fax: +46 8 524 81425.

ORCID

Nataliya K. Tarasova: 0000-0002-5816-277X

Didier Astruc: 0000-0001-6446-8751

Author Contributions

The manuscript was written through contributions of all authors. All authors have given approval to the final version of the manuscript. R.A.Z. has raised funding and had critical intellectual contribution to the conception of the study. N.K.T. conducted all the experiments, data acquisition, and analysis with assistance from A.G. and A.C. B.F. has significantly contributed to data interpretation and material support.

Funding

This work was supported by the European Commission (FP7-NANOSOLUTIONS, Grant Agreement No. 309329).

Notes

The authors declare no competing financial interest.

ACKNOWLEDGMENTS

The authors would like to acknowledge the help from the Proteomics Karolinska Core Facility (PK/KI) as well as from Amirata Saei Dibavar and Pierre Sabatiar at Karolinska Institutet. We thank the partners in WP3 and WP5 of the FP7-NANOSOLUTIONS consortium for providing the nanoparticle characterization.

ABBREVIATIONS

CNT, carbon nanotubes; DLS, dynamic light scattering; DSC, differential centrifugal sedimentation; EC50, half maximal effective concentration; GO, gene ontologies; LAL, Limulus amebocyte lysate; LPS, lipopolysaccharide; NF-κB, nuclear factor kappa-light-chain-enhancer of activated B cells; IκB-α, nuclear factor of kappa light polypeptide gene enhancer in B-cells inhibitor, alpha; NP, nanoparticles; OPLS, orthogonal projections to latent structures; PCA, principle component analysis; QD, quantum dots; TEM, transmission electron microscopy; TIPE2, tumor necrosis factor alpha-induced protein 8-like protein 2; TPP, thermal proteome profiling

REFERENCES

(1) Chang, Y.-N.; Zhang, M.; Xia, L.; Zhang, J.; Xing, G. The toxic effects and mechanisms of CuO and ZnO nanoparticles. *Materials* **2012**, *5* (12), 2850−2871.

(2) Ren, G.; Hu, D.; Cheng, E. W. C.; Vargas-Reus, M. a.; Reip, P.; Allaker, R. P. Characterisation of copper oxide nanoparticles for antimicrobial applications. *Int. J. Antimicrob. Agents* **2009**, *33* (6), 587−590.

DOI: 10.1021/acs.jproteome.6b00747
J. Proteome Res. 2017, 16, 689−697

(3) Jain, S.; Hirst, D. G.; O'Sullivan, J. M. Gold nanoparticles as novel agents for cancer therapy. *Br. J. Radiol.* **2012**, *85* (1010), 101−113.
(4) Rizvi, S. B.; Ghaderi, S.; Keshtgar, M.; Seifalian, A. M.; Muhammed, M. Semiconductor quantum dots as fluorescent probes for in vitro and in vivo bio-molecular and cellular imaging. *Nano Rev.* **2010**, *1*, 5161.
(5) Bhattacharya, K.; Mukherjee, S. P.; Gallud, A.; Burkert, S. C.; Bistarelli, S.; Bellucci, S.; Bottini, M.; Star, A.; Fadeel, B. Biological interactions of carbon-based nanomaterials: from coronation to degradation. *Nanomedicine* **2016**, *12* (2), 333−351.
(6) Chernobrovkin, A.; Marin-Vicente, C.; Visa, N.; Zubarev, R. A. Functional Identification of Target by Expression Proteomics (FITExP) reveals protein targets and highlights mechanisms of action of small molecule drugs. *Sci. Rep.* **2015**, *5*, 11176.
(7) Tarasova, N. K.; Ytterberg, A. J.; Lundberg, K.; Zhang, X.-M.; Harris, R. A.; Zubarev, R. A. Establishing a proteomics-based monocyte assay to assess differential innate immune activation responses. *J. Proteome Res.* **2016**, *15* (7), 2337−2345.
(8) Tsuchiya, S.; Yamabe, M.; Yamaguchi, Y.; Kobayashi, Y.; Konno, T.; Tada, K. Establishment and characterization of a human acute monocytic leukemia cell line (THP-1). *Int. J. Cancer* **1980**, *26* (2), 171−176.
(9) Franken, H.; Mathieson, T.; Childs, D.; Sweetman, G. M. A.; Werner, T.; Tögel, I.; Doce, C.; Gade, S.; Bantscheff, M.; Drewes, G.; Reinhard, F. B. M.; Huber, W.; Savitski, M. M. Thermal proteome profiling for unbiased identification of direct and indirect drug targets using multiplexed quantitative mass spectrometry. *Nat. Protoc.* **2015**, *10* (10), 1567−1593.
(10) Costa, P. M.; Fadeel, B. Emerging systems biology approaches in nanotoxicology: Towards a mechanism-based understanding of nanomaterial hazard and risk. *Toxicol. Appl. Pharmacol.* **2016**, *299*, 101−111.
(11) Haniu, H.; Matsuda, Y.; Takeuchi, K.; Kim, Y. A.; Hayashi, T.; Endo, M. Proteomics-based safety evaluation of multi-walled carbon nanotubes. *Toxicol. Appl. Pharmacol.* **2010**, *242* (3), 256−262.
(12) Yuan, J.; Gao, H.; Sui, J.; Duan, H.; Chen, W. N.; Ching, C. B. Cytotoxicity evaluation of oxidized single-walled carbon nanotubes and graphene oxide on human hepatoma HepG2 cells: An iTRAQ-coupled 2D LC−MS/MS proteome analysis. *Toxicol. Sci.* **2012**, *126* (1), 149−161.
(13) Palomäki, J.; Sund, J.; Vippola, M.; Kinaret, P.; Greco, D.; Savolainen, K.; Puustinen, A.; Alenius, H. A secretomics analysis reveals major differences in the macrophage responses towards different types of carbon nanotubes. *Nanotoxicology* **2015**, *9* (6), 719−728.
(14) Wuister, S. F.; Swart, I.; Van Driel, F.; Hickey, S. G.; de Mello Donega, C. Highly Luminescent Water-Soluble CdTe Quantum Dots. *Nano Lett.* **2003**, *3*, 503−507.
(15) Mazumder, S.; Dey, R.; Mitra, M. K.; Mukherjee, S.; Das, G. C. Review: Biofunctionalized quantum dots in biology and medicine. *J. Nanomater.* **2009**, *2009*, 1−17.
(16) Lovrić, J.; Cho, S. J.; Winnik, F. M.; Maysinger, D. Unmodified cadmium telluride quantum dots induce reactive oxygen species formation leading to multiple organelle damage and cell death. *Chem. Biol.* **2005**, *12* (11), 1227−1234.
(17) Wang, Z.; Li, N.; Zhao, J.; White, J. C.; Qu, P.; Xing, B. CuO nanoparticle interaction with human epithelial cells: Cellular uptake, location, export, and genotoxicity. *Chem. Res. Toxicol.* **2012**, *25* (7), 1512−1521.
(18) Pan, Y.; Neuss, S.; Leifert, A.; Fischler, M.; Wen, F.; Simon, U.; Schmid, G.; Brandau, W.; Jahnen-Dechent, W. Size-dependent cytotoxicity of gold nanoparticles. *Small* **2007**, *3* (11), 1941−1949.
(19) Goodman, C. M.; McCusker, C. D.; Yilmaz, T.; Rotello, V. M. Toxicity of gold nanoparticles functionalized with cationic and anionic side chains. *Bioconjugate Chem.* **2004**, *15* (4), 897−900.
(20) Lyutvinskiy, Y.; Yang, H.; Rutishauser, D.; Zubarev, R. a. In silico instrumental response correction improves precision of label-free proteomics and accuracy of proteomics-based predictive models. *Mol. Cell. Proteomics* **2013**, *12*, 2324−2331.
(21) Tarasova, N. K.; Ytterberg, A. J.; Lundberg, K.; Zhang, X.-M.; Harris, R. A.; Zubarev, R. A. Proteomics reveals a role for attachment in monocyte differentiation into efficient pro-inflammatory macrophages. *J. Proteome Res.* **2015**, *14* (9), 3940−3947.
(22) Benjamini, Y.; Hochberg, Y. Controlling the false discovery rate: a practical and powerful approach to multiple testing. *J. R. Stat. Soc. Ser. B* **1995**, *57* (1), 289−300.
(23) Cox, J.; Mann, M. MaxQuant enables high peptide identification rates, individualized p.p.b.-range mass accuracies and proteome-wide protein quantification. *Nat. Biotechnol.* **2008**, *26* (12), 1367−1372.
(24) Vallhov, H.; Qin, J.; Johansson, S. M.; Ahlborg, N.; Muhammed, M. A.; Scheynius, A.; Gabrielsson, S. The importance of an endotoxin-free environment during the production of nanoparticles used in medical applications. *Nano Lett.* **2006**, *6* (8), 1682−1686.
(25) Feliu, N.; Kohonen, P.; Ji, J. J.; Zhang, Y.; Karlsson, H. L.; Palmberg, L.; Nyström, A.; Fadeel, B. Next-generation sequencing reveals low-dose effects of cationic dendrimers in primary human bronchial epithelial cells. *ACS Nano* **2015**, *9* (1), 146−163.
(26) Pierce, J. W.; Schoenleber, R.; Jesmok, G.; Best, J.; Moore, S. a; Collins, T.; Gerritsen, M. E. Novel inhibitors of cytokine-induced IkappaBalpha phosphorylation and endothelial cell adhesion molecule expression show anti-inflammatory effects in vivo. *J. Biol. Chem.* **1997**, *272* (34), 21096−21103.
(27) Sun, H.; Gong, S.; Carmody, R. J.; Hilliard, A.; Li, L.; Sun, J.; Kong, L.; Xu, L.; Hilliard, B.; Hu, S.; Shen, H.; Yang, X.; Chen, Y. H. TIPE2, a negative regulator of innate and adaptive immunity that maintains immune homeostasis. *Cell* **2008**, *133* (3), 415−426.
(28) Sarkar, A.; Ravindran, G.; Krishnamurthy, V.; Campus, K. K. B. G. A brief review on the effect of cadmium toxicity: from cellular to organ level. *Int. J. Bio-Technology* **2013**, *3* (1), 17−36.
(29) Conroy, J.; Byrne, S. J.; Gun'ko, Y. K.; Rakovich, Y. P.; Donegan, J. F.; Davies, A.; Kelleher, D.; Volkov, Y. CdTe nanoparticles display tropism to core histones and histone-rich cell organelles. *Small* **2008**, *4* (11), 2006−2015.
(30) Villiers, C.; Freitas, H.; Couderc, R.; Villiers, M.-B.; Marche, P. Analysis of the toxicity of gold nano particles on the immune system: effect on dendritic cell functions. *J. Nanopart. Res.* **2010**, *12* (1), 55−60.
(31) Gerber, A.; Bundschuh, M.; Klingelhofer, D.; Groneberg, D. A. Gold nanoparticles: recent aspects for human toxicology. *J. Occup. Med. Toxicol.* **2013**, *8* (1), 32.
(32) Meng, H.; Xing, G.; Sun, B.; Zhao, F.; Lei, H.; Li, W.; Song, Y.; Chen, Z.; Yuan, H.; Wang, X.; Long, J.; Chen, C.; Liang, X.; Zhang, N.; Chai, Z.; Zhao, Y. Potent angiogenesis inhibition by the particulate form of fullerene derivatives. *ACS Nano* **2010**, *4* (5), 2773−2783.
(33) Miao, Y.; Xu, J.; Shen, Y.; Chen, L.; Bian, Y.; Hu, Y.; Zhou, W.; Zheng, F.; Man, N.; Shen, Y.; Zhang, Y.; Wang, M.; Wen, L. Nanoparticle as signaling protein mimic: robust structural and functional modulation of CaMKII upon specific binding to fullerene C60 nanocrystals. *ACS Nano* **2014**, *8* (6), 6131−6144.
(34) Gallud, A.; Fadeel, B. Keeping it small: towards a molecular definition of nanotoxicology. *Eur. J. Nanomed.* **2015**, *7* (3), 143−151.

DOI: 10.1021/acs.jproteome.6b00747
J. Proteome Res. 2017, 16, 689−697